RECONSTRUCTION FOR STOCHASTIC 3-D SIGNALS WITH SYMMETRIC STATISTICS IN NOISE: ELECTRON MICROSCOPY OF VIRUS PARTICLES

Nan Xu and Peter C. Doerschuk

School of Electrical and Computer Engineering, Cornell University, Ithaca, NY, USA

ABSTRACT

Cryo electron microscopy leads to 3-D image reconstruction problems. The data is one projection of each of many different instances of the object. When the object has symmetry and is also heterogeneous, it is natural to describe the object as stochastic with symmetrical statistics. This paper describes methods for incorporating the symmetry into expectation-maximization algorithms for the maximum likelihood solution of the reconstruction problem.

Index Terms— cryo electron microscopy, viruses, symmetrical statistics, maximum likelihood reconstruction

1. INTRODUCTION

An important approach to studying biological nanomachines (e.g., viruses and ribosomes) is structural biology, which focuses on the geometric shape of the particle at resolutions as small as atomic resolution and on the relationship between geometry and biological function. An increasingly important technique is single-particle cryo electron microscopy (cryo EM). In cryo EM, a specimen containing thousands of particles is flash frozen to cryogenic temperatures and imaged. The physics is such that the image is basically a highly-noisy (SNR < 0.1) 2-D projection of the 3-D electron scattering intensity distribution of the particle. However, for various technical reasons, only one projection is taken and the orientation of the projection direction is unknown. So, instead of reconstructing based on a full set of oriented projection images of a single particle, as is done in x-ray computed tomography in medical imaging, many images each of different instances of the particle and with different and unknown projection directions much be computationally combined to compute the reconstruction [1]. Standard approaches assume that the particles are either identical or are members of a small number of discrete classes such that all particles in a class are identical. In [2, 3], we demonstrated an approach to reconstruction which includes both discrete classes and continuous variability of the particles within each class.

Many viruses of both animals and plants belong to the class of "spherical" viruses for which case the virus particle

has a shell of protein, called a "capsid", surrounding a cavity containing the viral genome. Typical sizes and molecular weights of the virus particles are 10^2–10^3Å and 10MDa. The capsid is constructed of many repetitions of the same peptide molecule in geometric arrays similar to human-constructed geodesic domes. The capsid has a geometric symmetry, of which the most common is icosahedral symmetry (i.e., the symmetries of the icosahedron whose surface is 20 equilateral triangles and which has 2-fold rotational symmetry axes at the midpoint of each edge of each triangle, 3-fold rotational symmetry axes at the center of each triangle, and 5-fold rotational symmetry axes at each vertex of each triangle for a total of 60 symmetry operations). Focus on the virus particles within one class. The standard view is that each instance of the virus particle is identical and exactly obeys the symmetry. An intermediate view is that the different instances are different (due, for example, to the inherent flexibility of such a large molecular complex) but still each instance exactly obeys the symmetry [2, 3]. This paper considers a more sophisticated view which is that the different instances of the particle are different and that it is the statistics of the particle that obey the symmetry not the individual particles.

Conditional on class membership, each particle can be described as a linear combination of basis functions where the weights in the linear combination are Gaussian random variables [2, 3]. Because the viral particles are roughly spherical in shape and the icosahedral symmetry is a rotational symmetry, it is natural to use spherical coordinates ($\mathbf{x} = (x, \theta, \phi)$). Because of the group theory, it is natural to use vector valued angular basis functions $I_\zeta(\theta, \phi)$ or equivalently $I_\zeta(\mathbf{x}/x)$ and therefore vector valued radially-dependent weights $c_\zeta(x)$ so that the weighted linear combination of basis functions has the form

$$\rho(\mathbf{x}) = \sum_\zeta I_\zeta^T(\mathbf{x}/x)c_\zeta(x) \tag{1}$$

where $\rho(\mathbf{x})$ is the electron scattering intensity of a virus particle, and ^{T} is transpose. Because $\rho(\cdot)$ is real, it is convenient to have real-valued basis functions and weights.

The goal of the maximum likelihood (ML) reconstruction procedure is to determine the mean vector and covariance matrix of the vector of weights $c_\zeta(x)$, which is a generalization of classical ML Gaussian mixture parameter estimation [4]. Our current software running on a desktop PC

can solve problems with about 10^3 weights. Because of the Gaussian assumption, only the behavior of the first two moments need to be specified and the natural specification is [3] $\bar{\rho}(R_g^{-1}\mathbf{x}) = \bar{\rho}(\mathbf{x})$ and $R_\rho(R_g^{-1}\mathbf{x}_1, R_g^{-1}\mathbf{x}_2) = R_\rho(\mathbf{x}_1, \mathbf{x}_2)$ where $\bar{\rho}(\cdot)$ is the mean function and $R_\rho(\cdot, \cdot)$ is the correlation function of the electron scattering intensity $\rho(\cdot)$, $R_g \in \mathbb{R}^{3\times 3}$ is the gth rotation matrix of the symmetry group, and $\mathbf{x}, \mathbf{x}_1, \mathbf{x}_2 \in \mathbb{R}^3$. Choosing basis functions and determining conditions on the weights which guarantee $\bar{\rho}(R_g^{-1}\mathbf{x}) = \bar{\rho}(\mathbf{x})$ is straightforward [3]. But the condition $R_\rho(R_g^{-1}\mathbf{x}_1, R_g^{-1}\mathbf{x}_2) = R_\rho(\mathbf{x}_1, \mathbf{x}_2)$ is more challenging and is the subject of this paper.

2. REAL-VALUED ANGULAR BASIS FUNCTIONS

It is necessary to have a set of angular basis functions that are a complete orthonormal system on the surface of the sphere. Looking forward to Section 3, it is convenient to have each basis function possess well-characterized transformation properties under the rotations of the symmetry group. The natural way to achieve these two objectives is to use angular basis functions that transform as one of the irreducible representations (irred reps) of the group. A standard group theory approach to determine such basis functions is to apply projection operators to the spherical harmonics [5, p. 93].

2.1. Projections of spherical harmonics and construction of a basis

Because the symmetry group is finite, the projection operator $\mathcal{P}_{\mu,\nu}^p$ applied to a function $\psi(\mathbf{x})$ is a weighted sum of symmetry operators $P(g)$ applied to $\psi(\mathbf{x})$ where the weights are matrix elements of an irred rep and, for rotational operations, $P(g)\psi(\mathbf{x}) = \psi(R_g^{-1}\mathbf{x})$:

$$\mathcal{P}_{\mu,\nu}^p \psi(\mathbf{x}) = \frac{d_p}{N_g} \sum_{g \in G} \Gamma^p(g)_{\mu,\nu}^* P(g)\psi(\mathbf{x}) \qquad (2)$$

where G is the group having N_g elements denoted by g, $\Gamma^p(g)$ is the matrix corresponding to group element g in the pth irred rep of the group ($p \in \{1, \ldots, N_{\text{rep}}\}$), and d_p is the dimension of $\Gamma^p(g)$. For the icosahedral group, $N_g = 60$ and $N_{\text{rep}} = 5$.

Because spherical harmonics, denoted by $Y_{l,m}(\mathbf{x}/x)$ ($l \in \mathbb{N}$, $m \in \{-l, \ldots, +l\}$), form a complete orthonormal basis on the surface of the sphere and have simple properties under rotation, we choose to use $\psi(\mathbf{x}) = Y_{l,m}(\mathbf{x}/x)$. The rotational property of $Y_{l,m}$ is

$$Y_{l,m}\left(R_g^{-1}\frac{\mathbf{x}}{x}\right) = \sum_{m'=-l}^{+l} D_{m',m}^l(\alpha(g), \beta(g), \gamma(g)) Y_{l,m'}\left(\frac{\mathbf{x}}{x}\right) \qquad (3)$$

where $D_{m',m}^l(\alpha(g), \beta(g), \gamma(g))$ is the Wigner D coefficient depending on $(\alpha(g), \beta(g), \gamma(g))$ which are the Euler angles of rotation at element g. Therefore, the projection operator applied to a spherical harmonic can be expressed in the form

$$\mathcal{P}_{\mu,\nu}^p Y_{l,m}\left(\frac{\mathbf{x}}{x}\right) = \sum_{m'=-l}^{+l} \mathcal{D}_{\mu,\nu,l,m,m'}^p(g) Y_{l,m'}\left(\frac{\mathbf{x}}{x}\right) \qquad (4)$$

where

$$\mathcal{D}_{\mu,\nu,l,m,m'}^p(g) = \frac{d_p}{N_g} \sum_{g \in G} \Gamma^p(g)_{\mu,\nu}^* D_{m',m}^l(\alpha(g), \beta(g), \gamma(g)). \qquad (5)$$

Eqs. 4–5 can be used to compute a set of functions that spans the subspace (degree l and irred rep p) by Algorithm 1. However, the number of functions is more than is needed for a basis. Specifically, for each l, Algorithm 1 provides $2l+1$ d_p-dimensional vectors of basis functions by varying m through the set $\{-l, \ldots, +l\}$. Therefore, the final basis of dimension $N_{p;l} \le 2l + 1$ is obtained by orthogonalizing the set of functions.

Algorithm 1: Construct orthonormal basis functions for a finite group where $p \in \{1, \ldots, N_{\text{rep}}\}$, $l \in \mathbb{N}$, and $m \in \{-l, \ldots, +l\}$.

Data: $Y_{l,m}(\frac{\mathbf{x}}{x})$, Γ^p, $D_{m',m}^l$
Result: a $d_p \times 1$ vector of basis functions, $I_{p;l,m}(\frac{\mathbf{x}}{x})$

1 **for** $i = 1$; $i <= d_p$; $i++$ **do**
2   compute $\psi_{p,i;l,m}(\frac{\mathbf{x}}{x}) = \mathcal{P}_{i,i}^p Y_{l,m}(\frac{\mathbf{x}}{x})$ from Eq. 4 and then $c_{p,i;l,m} = \|\psi_{p,i;l,m}(\frac{\mathbf{x}}{x})\|_2$
3   **if** $c_{p,i;l,m} \neq 0$ **then**
4          $I_{p;l,m}(\frac{\mathbf{x}}{x})[i] = \frac{1}{c_{p,i;l,m}}\psi_{p,i;l,m}(\frac{\mathbf{x}}{x})$, the ith entry of vector $I_{p;l,m}(\frac{\mathbf{x}}{x})$
5   **for** $j = 1$; $j <= d_p$, $j \neq i$; $j++$ **do**
6              $I_{p;l,m}(\frac{\mathbf{x}}{x})[j] = (\frac{1}{c_{p,i;l,m}})\mathcal{P}_{j,i}^p Y_{l,m}(\frac{\mathbf{x}}{x})$, computed from Eq. 4
7   **end**
8   break;
9   **else**
10   continue;
11   **end**
12 **end**

2.2. Computing a real-valued basis

Because the electron scattering intensity $\rho(\mathbf{x})$ is real and there are natural real-valued radial basis functions, it is convenient to have real-valued angular basis functions $I_\zeta(\mathbf{x}/x)$, since then the weights $c_\zeta(x)$ are also real valued. One approach to determining real-valued angular basis functions is to use irred reps that are real. In this case, the imaginary part of the weights $\mathcal{D}_{\mu,\nu,l,m,m'}^p(g)$ and the imaginary part of spherical harmonics $Y_{l,m'}(\frac{\mathbf{x}}{x})$ in Eq. 4 can be cancelled out.

For each of the N_{rep} possible irred reps of the icosahedral group G, Liu, Ping, and Chen [6] give a set of N_g complex-valued unitary matrices denoted by Γ_c^p for $p \in \{1, \ldots, N_{\text{rep}}\}$. Let $\chi^p(g)$ be the character of element $g \in G$ in the irred rep Γ_c^p, i.e., the trace of Γ_c^p. For all p sets of Γ_c^p, $1/N_g \sum_{g \in G} \chi^p(g)^2 = 1$. Therefore, by Theorem II and III in Ref. [5, p. 128-129], it follows that there exist equivalent irred reps for the icosahedron group with real-valued matrices, denoted by Γ_r^p, and such real unitary irred rep matrices can be computed by a similarity transformation from

the complex matrices provided by Liu, Ping, and Chen [6], i.e., $\Gamma_r^p(g) = (S^p)^T \Gamma_c^p(g) S^p$ with some unitary matrix S^p for $p \in \{1, \dots, N_{\text{rep}}\}$. We have done this and the algorithm, software, and numerical values of the S^p matrices are available from the authors.

Computation of $\mathcal{D}_{\mu,\nu,l,m,m'}^p$ (Eq. 5) requires computation of Wigner D coefficients which in turn require knowledge of the Euler angles describing the rotation corresponding to each element of the group. These angles are not unique, since if the icosahedron is positioned in different orientations, the symmetry rotations (and therefore the Euler angles) are typically different. Zheng and Doerschuk [7] give a 3-D irred rep of the icosahedral group which is exactly the symmetry rotation matrices for an icosahedron that is positioned in a standard orientation (the z axis passes through two opposite vertices and the xz plane includes one edge of the icosahedron). In order to use the corresponding Euler angles in Eq. 5, a permutation of the Zheng and Doerschuk [7] irred rep was determined so that the resulting multiplication table matched the table of Liu, Ping, and Chen [6] and such that there was a similarity transformation between the permuted Zheng and Doerschuk [7] irred rep and the $p = 2$ Liu, Ping, and Chen [6] irred rep. The permuted irred rep is denoted by R_g ($g \in \{1, \dots, N_g\}$). The algorithm and numerical results are available upon request.

With the five real-valued irred reps and the Euler angles of the previous two paragraphs, first $\mathcal{D}_{\mu,\nu,l,m,m'}^p$ (Eq. 5) and then the complete set of angular basis functions, denoted by $I_{p;l,n}(\mathbf{x}/x)$ where $n \in \{1, \dots, N_{p;l}\}$, can be computed. For visualization purposes, define the 3-D object $\xi(\mathbf{x})$ by

$$\xi(\mathbf{x}) = \begin{cases} 1, & x \le \kappa_1 + \kappa_2 I_{p;l,n}(\mathbf{x}/x) \\ 0, & \text{otherwise} \end{cases} \quad (6)$$

where κ_1 and κ_2 are chosen so that $\kappa_1 + \kappa_2 I_{p;l,n}(\mathbf{x}/x)$ varies between 0.5 and 1. Examples are shown in Figure 1. These calculations have been verified in several ways. The number of basis functions in the subspace of square integrable functions on the surface of the sphere which is defined by a fixed value of l has dimension $2l + 1$. The number of functions resulting from the orthogonalization, when summed over all p values, has been verified to be $2l + 1$ as expected. The d_p-dimensional vector basis functions are expected to have a specific transformation property under rotations from the group [5, p. 20], in particular,

$$I_{p;l,n}(R_g^{-1}\mathbf{x}/x) = (\Gamma_r^p(g))^T I_{p;l,n}(\mathbf{x}/x), \quad (7)$$

which has also been verified. Note that this is transpose instead of Hermitian transpose.

3. SYMMETRY CAUSES CONSTRAINTS ON THE COVARIANCE MATRIX

Achieving $R_\rho(R_g^{-1}\mathbf{x}, R_g^{-1}\mathbf{x}') = R_\rho(\mathbf{x}, \mathbf{x}')$ requires constraints on the second order statistics of the radially-dependent
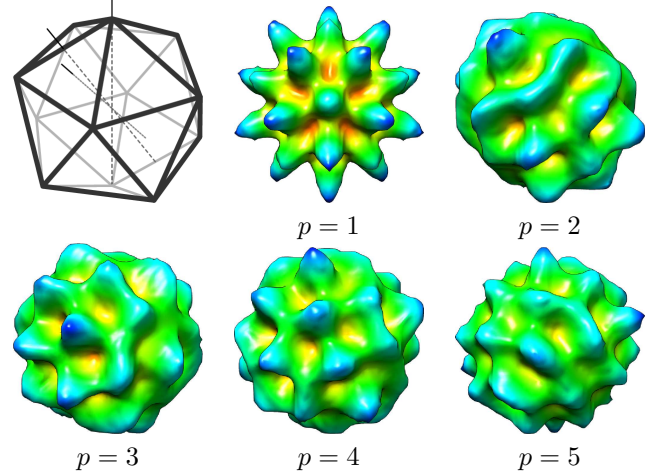

Fig. 1: An icosahedron with one of each type of symmetry axis (2-, 3-, and 5-fold) shown and example angular basis functions with $l = 10$ and $p \in \{1, \dots N_{\text{rep}}\}$. The surfaces of 3-D objects defined by Eq. 6 are visualized by UCSF Chimera where the color indicates the distance from the center of the object. Note that $p = 1$ exhibits all of the symmetries of an icosahedron.

weights $c_\zeta(x)$ in the orthonormal expansion (Eq. 1) that represents the electron scattering intensity where ζ is shorthand for $p; l, n$.

3.1. Concrete form for the symmetry constraint

By definition, $R_\rho(\mathbf{x}, \mathbf{x}') = \mathbb{E}\left[\rho(\mathbf{x})\rho^T(\mathbf{x}')\right]$. Use Eq. 1 twice and simplify. Do the same for $R_\rho(R_g^{-1}\mathbf{x}, R_g^{-1}\mathbf{x}')$ by using the transformation property (Eq. 7). Then equating the two expressions gives the requirement that

$$\sum_\zeta \sum_{\zeta'} I_\zeta^T\left(\frac{\mathbf{x}}{x}\right) \mathbb{E}\left[c_\zeta(x)c_{\zeta'}^T(x')\right] I_{\zeta'}\left(\frac{\mathbf{x}'}{x'}\right)$$

$$= \sum_\zeta \sum_{\zeta'} I_\zeta^T\left(\frac{\mathbf{x}}{x}\right)(\Gamma_f^p(g))^T \mathbb{E}\left[c_\zeta(x)c_{\zeta'}^T(x')\right] \Gamma_f^p(g) I_{\zeta'}\left(\frac{\mathbf{x}'}{x'}\right)$$

for all $g \in \{1, \dots, N_g\}$. On both sides, multiply on the left by $I_{\zeta_1}(\mathbf{x}/x)$ and on the right by $I_{\zeta_2}^T(\mathbf{x}'/x')$ and integrate over the surface of the $\mathbf{x}$ and $\mathbf{x}'$ spheres. Since the basis functions are orthonormal on the surface of the sphere, this implies that

$$\mathbb{E}\left[c_{\zeta_1}(x)c_{\zeta_2}^T(x')\right] = (\Gamma^{p_1}(g))^T \mathbb{E}\left[c_{\zeta_1}(x)c_{\zeta_2}^T(x')\right] \Gamma^{p_2}(g).$$

Therefore, since the irred rep is unitary ($\Gamma^p(g)^{-1} = \Gamma^p(g)^T$), it follows that

$$\Gamma^{p_1}(g)\mathbb{E}\left[c_{\zeta_1}(x)c_{\zeta_2}^T(x')\right] = \mathbb{E}\left[c_{\zeta_1}(x)c_{\zeta_2}^T(x')\right] \Gamma^{p_2}(g) \quad (8)$$

for all $g \in \{1, \dots, N_g\}$, $x, x' \ge 0$, $p_1, p_2 \in \{1, \dots, N_{\text{rep}}\}$, $l_1, l_2 \in \{0, 1, \dots\}$, $n_1 \in \{1, \dots, N_{p_1;l_1}\}$, and $n_2 \in \{1, \dots, N_{p_2;l_2}\}$.

To make this work suitable for computation, the radially-dependent weights are expressed as an orthonormal expansion in the form $c_\zeta(x) = \sum_{q=1}^\infty c_{\zeta,q} h_{l,q}(x)$ where both $c_{\zeta,q}$ and

$h_{l,q}(x)$ are real-valued and the radial basis $h_{l,q}(x)$ is exactly the family of functions used in Ref. [8, Section IIIB] with the orthonormality condition $\int_{r=0}^{\infty} h_{l,q}(x)h_{l,q'}(x)x^2 \mathrm{d}x = \delta_{q,q'}$. Use the orthonormal expansion twice on both sides of Eq. 8, multiply both sides by $h_{l_1,q}(x)h_{l_2,q'}(x')$, and integrate x and x' on $[0,\infty)$ with integration measure $x^2 x'^2 \mathrm{d}x \mathrm{d}x'$ to get $\Gamma^{p_1}(g)\mathbb{E}\left[c_{\zeta_1,q}c_{\zeta_2,q'}^T\right] = \mathbb{E}\left[c_{\zeta_1,q}c_{\zeta_2,q'}^T\right]\Gamma^{p_2}(g)$ which must be true for all $g \in \{1, \ldots, N_g\}$, $q, q' \in \{1, 2, \ldots\}$, $p_1, p_2 \in \{1, \ldots, N_{\mathrm{rep}}\}$, $l_1, l_2 \in \{0, 1, \ldots\}$, $n_1 \in \{1, \ldots, N_{p_1;l_1}\}$, and $n_2 \in \{1, \ldots, N_{p_2;l_2}\}$. Note that its solution for $\mathbb{E}\left[c_{\zeta_1,q}c_{\zeta_2,q'}^T\right]$ does not depend on ζ_1, q, ζ_2, and q' except that unspecified degrees of freedom in the solution could depend on ζ_1, q, ζ_2, and q'. Therefore, the above equation can be simplified to

$$\Gamma^{p_1}(g)V_{p_1:p_2} = V_{p_1:p_2}\Gamma^{p_2}(g) \tag{9}$$

for some $d_{p_1} \times d_{p_2}$ matrix $V_{p_1:p_2}$, which must be true for all $g \in \{1, \ldots, N_g\}$ and $p_1, p_2 \in \{1, \ldots, N_{\mathrm{rep}}\}$.

Then, the problem is to determine the form of the matrix $V_{p_1:p_2}$ to solve Eq. (9), with the additional constraint that its sub-blocks must be a real-valued positive semidefinite matrix since it is a covariance matrix and the $c_{\zeta,q}$ vectors are actually real valued.

3.2. Solution of the symmetry constraint

Eq. 9 has substantial structure because the $\Gamma^{p_2}(g)$ are an irred rep. Schur's Lemma [5, Theorem I and II, Section 4.5, p. 80] and related results imply that

$$V_{p_1:p_2} = \begin{cases} v_{p_1}((l_1,n_1,q_1),(l_2,n_2,q_2))I_{d_{p_1}}, & p_1 = p_2 \\ \mathbf{0}_{d_{p_1},d_{p_2}}, & \text{otherwise} \end{cases}$$

where $\mathbf{0}_{i,j}$ is the $i \times j$ zero matrix.

The covariance matrix V constructed from all of the $\mathbb{E}\left[c_{\zeta_1,q}c_{\zeta_2,q'}^T\right]$ sub-blocks must be a real-valued positive semidefinite matrix. Recall that this is a structured situation since the solution for $\mathbb{E}\left[c_{\zeta_1,q}c_{\zeta_2,q'}^T\right]$ depends explicitly on p_1 and p_2 but depends on l_1, n_1, q_1, l_2, n_2, q_2 only through the unspecified degree of freedom of $\mathbb{E}\left[c_{\zeta_1,q}c_{\zeta_2,q'}^T\right]$. Suppose that the indices vary from slowest to fastest in the order p, l, n, and q. Let the number of triples of (l,n,q) be $N_{\zeta,q}$. To simplify notation, let $\alpha \in \{1, \ldots, N_{\zeta,q}\}$ represent the (l,n,q) indices. Then p is constant over sequential sets of $d_p N_{\zeta,q}$ rows and columns. Therefore the entire covariance matrix V is block diagonal with five blocks, corresponding to the five values of p. The pth block itself is organized into subblocks (themselves diagonal) with value $v_p((l_1,n_1,q_1),(l_2,n_2,q_2))I_{d_p}$ which are not specified by Eq. 9. So the pth block is of the form $V_{p:p} =$

$$\begin{bmatrix} v_p(1,1)I_{d_p} & v_p(1,2)I_{d_p} & \ldots & v_p(1,N_{\zeta,q})I_{d_p} \\ v_p(2,1)I_{d_p} & v_p(2,2)I_{d_p} & \ldots & v_p(2,N_{p;l,n,q})I_{d_p} \\ \vdots & \vdots & \ddots & \vdots \\ v_p(N_{\zeta,q},1)I_{d_p} & v_p(N_{\zeta,q},2)I_{d_p} & \ldots & v_p(N_{\zeta,q},N_{\zeta,q})I_{d_p} \end{bmatrix} \tag{10}$$

where $v_p(i,j) = v_p(\alpha_1 = i, \alpha_2 = j)$ for $i, j \in \{1, ..., N_{\zeta,q}\}$ and $p \in \{1, ..., N_{\mathrm{rep}}\}$.

A block-diagonal matrix can be a real-valued positive semidefinite matrix if and only if each of the blocks is a real-valued positive semidefinite matrix. In order to have Eq. 10 be a real-valued positive semidefinite matrix it is necessary that $v_p(i,i) \geq 0$ for $i \in \{1, ..., N_{\zeta,q}\}$ and $p \in \{1, ..., N_{\mathrm{rep}}\}$. In addition, the off diagonal terms must decrease sufficiently quickly.

4. FUTURE WORK

We are currently revising the software of Ref. [3] to include the basis functions of Section 2, the constraint on the second moments $\mathbb{E}\left[c_{\zeta_1,q}c_{\zeta_2,q'}^T\right]$ of the weights $c_{\zeta,q}$ from Section 3, and various related changes (e.g., change the integration rule in the expectation-maximization algorithm that computes the ML estimate of the weights $c_{\zeta,q}$) which will enable the software to solve these important electron microscopy image reconstruction problems with a complete treatment of the symmetry of the virus object which is a completely novel addition to computational structural biology.

5. REFERENCES

[1] Grant J. Jensen, Ed., *Cryo-EM, Parts A–C*, vol. 481–483 of *Methods in Enzymology*, Elsevier Inc., 2010.

[2] Qiu Wang, Tsutomu Matsui, Tatiana Domitrovic, Yili Zheng, Peter C. Doerschuk, and John E. Johnson, "Dynamics in cryo EM reconstructions visualized with maximum-likelihood derived variance maps," *J. Struct. Biol.*, vol. 181, no. 3, pp. 195–206, Mar. 2013.

[3] Yili Zheng, Qiu Wang, and Peter C. Doerschuk, "3-D reconstruction of the statistics of heterogeneous objects from a collection of one projection image of each object," *J. Opt. Soc. Am. A*, vol. 29, no. 6, pp. 959–970, June 2012.

[4] Richard A. Redner and Homer F. Walker, "Mixture densities, maximum likelihood and the EM algorithm," *SIAM Review*, vol. 26, no. 2, pp. 195–239, Apr. 1984.

[5] J. F. Cornwell, *Group Theory in Physics*, vol. 1, Academic Press, London, 1984.

[6] Fa Liu, Jia-Lun Ping, and Jin-Quan Chen, "Application of the eigenfunction method to the icosahedral group," *J. Math. Phys.*, vol. 31, no. 5, pp. 1065–1075, 1990.

[7] Yibin Zheng and Peter C. Doerschuk, "Symbolic symmetry verification for harmonic functions invariant under polyhedral symmetries," *Comput. in Phys.*, vol. 9, no. 4, pp. 433–437, July/August 1995.

[8] Yibin Zheng and Peter C. Doerschuk, "3D image reconstruction from averaged Fourier transform magnitude by parameter estimation," *IEEE Transactions on Image Processing*, vol. 7, no. 11, pp. 1561–1570, Nov. 1998.